Journal of Maps

ISSN: (Print) 1744-5647 (Online) Journal homepage: https://www.tandfonline.com/loi/tjom20

Structural and metallogenic map of late Variscan Arbus Pluton (SW Sardinia, Italy)

Stefano Cuccuru, Stefano Naitza, Francesco Secchi, Antonio Puccini, Leonardo Casini, Pamela Pavanetto, Ulf Linnemann, Mandy Hofmann & Giacomo Oggiano

To cite this article: Stefano Cuccuru, Stefano Naitza, Francesco Secchi, Antonio Puccini, Leonardo Casini, Pamela Pavanetto, Ulf Linnemann, Mandy Hofmann & Giacomo Oggiano (2016) Structural and metallogenic map of late Variscan Arbus Pluton (SW Sardinia, Italy), Journal of Maps, 12:5, 860-865, DOI: 10.1080/17445647.2015.1091750

To link to this article: https://doi.org/10.1080/17445647.2015.1091750

JOURNAL OF MAPS, 2016
VOL. 12, NO. 5, 860–865
http://dx.doi.org/10.1080/17445647.2015.1091750

Taylor & Francis
Taylor & Francis Group

SCIENCE

Structural and metallogenic map of late Variscan Arbus Pluton (SW Sardinia, Italy)

Stefano Cuccuru[a], Stefano Naitza[b], Francesco Secchi[a], Antonio Puccini[a], Leonardo Casini[a], Pamela Pavanetto[c], Ulf Linnemann[d], Mandy Hofmann[d] and Giacomo Oggiano[a]

[a]Dipartimento di Scienze della Natura e del Territorio (DipNeT), University of Sassari, Sassari, Italy; [b]Dipartimento di Ingegneria Civile, Ambientale e Architettura (DICAAR), University of Cagliari, Cagliari, Italy; [c]Dipartimento di Scienze della Terra (DISTER), University of Cagliari, Cagliari, Italy; [d]Sektion Geochronologie, Senckenberg Naturhistorische Sammlungen Dresden, Museum für Mineralogie und Geologie, Dresden, Germany

ABSTRACT

This paper presents the geological, structural and metallogenic map of the Arbus Pluton, a late Variscan composite intrusion belonging to the Corsica-Sardinia Batholith. The pluton is surrounded and crosscut by a wide variety of vein ore deposits. The Arbus Pluton was emplaced at shallow crustal levels at the end of the Variscan Orogeny, along an E–W trending shear zone located in the low-grade external nappe pile of the Sardinian basement. The architecture of the pluton is roughly concentric with a core of cordierite-bearing leucogranites and an outer shell composed of pyroxene-bearing and hornblende granodiorites. New U/Pb dating on zircons of granodiorite yields an emplacement age of 303.7 ± 1.1 which improves previous Rb/Sr and Ar/Ar dating. The map has been compiled on the basis of new geological/structural surveys and petrographical studies coupled with *in situ* gamma ray spectrometry. All the data-sets have been processed using a geographical information system.

ARTICLE HISTORY
Received 12 February 2015
Revised 21 August 2015
Accepted 4 September 2015

KEYWORDS
Variscan orogeny; Corsica–Sardinia Batholith; granite-related ore deposits

1. Introduction

The Paleozoic basement of Sardinia (Figure 1) is part of the Southern Variscan Belt (Rossi, Oggiano, & Cocherie, 2009). At the end of the orogeny, the development of a large thermal anomaly probably related to shear heating along lithospheric-scale faults (Casini, Puccini, Cuccuru, Maino, & Oggiano, 2013; Maino et al., 2015) led to the emplacement of a large number of calcalkaline plutons that collectively form the Corsica-Sardinia Batholith (Bralia, Ghezzo, Guasparri, & Sabatini, 1981; Carmignani, Carosi, et al., 1994; Casini, Cuccuru, Puccini, Oggiano, & Rossi, 2015; Ferré & Leake, 2001; Rossi & Cocherie, 1991). The magmatic activity lasted between 340 and 285 Ma (Cocherie, Rossi, Fanning, & Guerrot, 2005; Paquette, Ménot, Pin, & Orsini, 2003). According to Cocherie et al. (2005), building the batholith involved three main episodes corresponding to three different magmatic suites: (i) the oldest Mg-K suite (U1) formed between 340 and 336 Ma, (ii) the calcalkaline suite (U2) between 320 and 290 Ma (Casini, Cuccuru, Maino, et al., 2015; Casini, Cuccuru, Maino, Oggiano, & Tiepolo, 2012) and (iii) a late-Variscan composite suite (U3) including alkaline and layered tholeitic bodies mostly emplaced around 285 Ma (Casini et al., 2015; Gaggero, Oggiano, Buzzi, Slejko, & Cortesogno, 2007; Paquette et al., 2003). Despite the recent improvement of geochronological and geochemical data, the knowledge of the Sardinia portion of the batholith is still far from complete, as large areas, they lack detailed geological and structural field mapping. In southwestern Sardinia, a good example of composite pluton is represented by the Arbus Pluton. Past studies (Secchi, Brotzu, & Callegari, 1991) evidenced a mafic to felsic evolution dominated by crystal/liquid fractionation, in contrast with the processes documented for most igneous sequences of northern Sardinia (Bralia et al., 1981; Poli, Ghezzo, & Conticelli, 1989; Zorpi, Coulon, & Orsini, 1991). The Arbus Pluton is associated with a large hydrothermal vein network (Montevecchio–Ingurtosu–Gennamari district), already described in detailed but outdated papers (Cavinato & Zuffardi, 1948; Dessau, 1935, 1936; Zuffardi, 1958).

2. Methods

2.1. *Structural analysis*

Magmatic flow trajectories in the Arbus Pluton were deduced by measuring the prevailing shape and preferred orientation of elongated metamorphic xenoliths and micro-granular mafic enclaves. Poles to foliation were projected in stereoplots to obtain information about the geometry of the pluton and the emplacement mechanism.

CONTACT Stefano Cuccru scuccuru@uniss.it

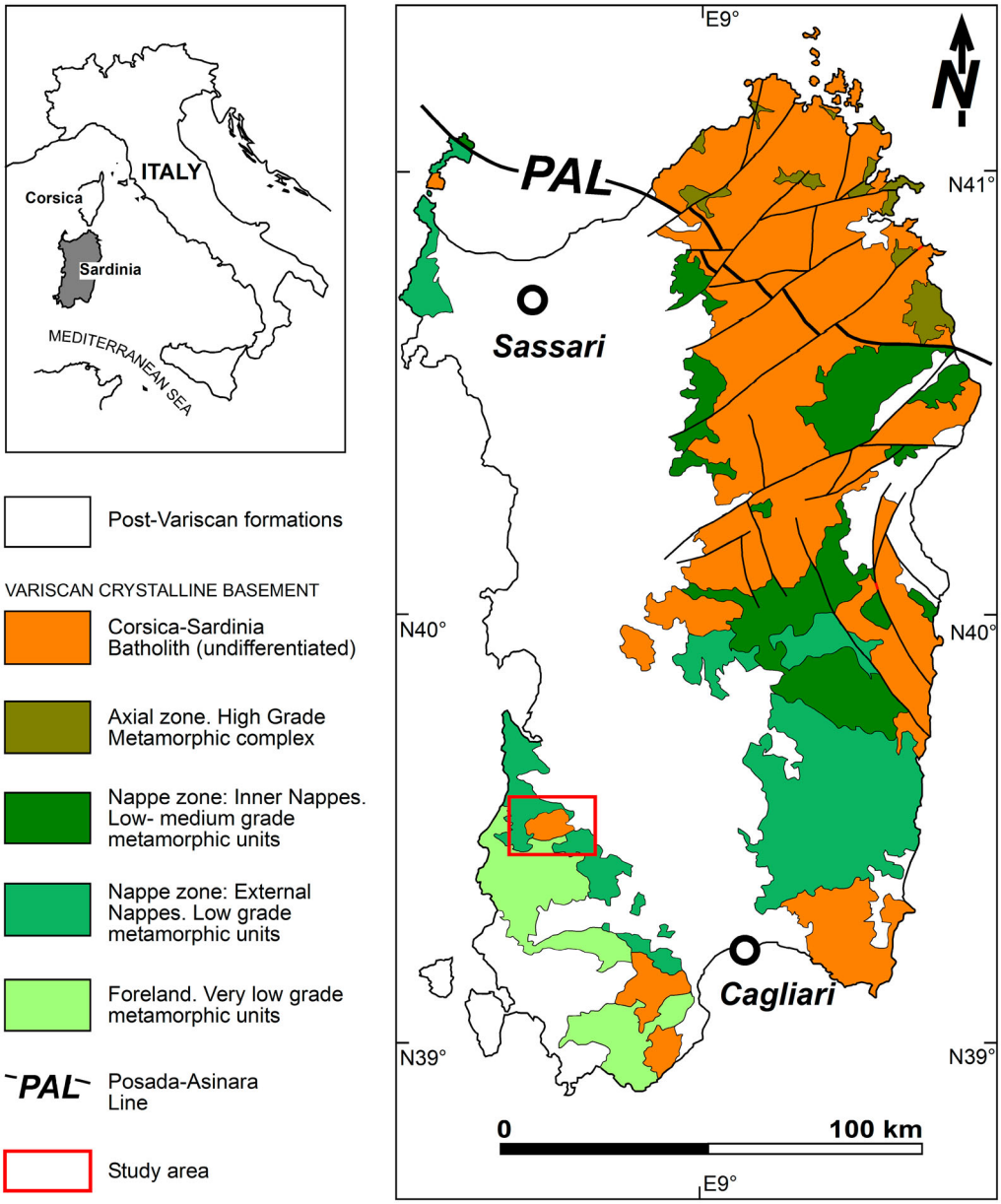

Figure 1. Geological sketch map of the Variscan basement of Sardinia. Red square indicates the study area.

2.2. *Remote sensing*

A digital elevation model (DEM; Friese, Vollbrecht, Tanner, Fahlbusch, & Weidemann, 2011) was created from a mosaic of 1:10,000 topographic maps. The DEM was integrated with geo-referenced high-resolution aerial orthophotos (property of Regione Autonoma della Sardegna) and IKONOS 2005 satellite images. Results were processed using Matlab software to boost geomorphological features related to major faults, joints networks and lithological boundaries within the composite pluton. Data were finally processed in a geographical information system and a map produced.

2.3. *Gamma ray spectrometry*

Specific activities of ^{40}K, ^{238}U and ^{232}Th were measured using a portable gamma ray spectrometer in 32 representative outcrops (Table 1) of magmatic and surrounding metamorphic rocks, following the procedure reported in Puccini et al. (2014) and references therein. Also these data were processed using a Matlab-derived script in order to confirm the internal compositional changes of the pluton.

Table 1. Median values of the log-normal distribution of ^{40}K, ^{238}U, ^{232}Th concentration with 1σ asymmetrical uncertainty, based on 32 measurements carried out with portable gamma ray spectrometer.

Rock type	Sample	^{40}K (%)	^{238}U (ppm)	^{232}Th (ppm)
MG	2	$1.75^{+0.38}_{-0.31}$	$1.88^{+0.12}_{-0.11}$	$7.27^{+0.88}_{-0.79}$
GD	15	$3.15^{+0.47}_{-0.41}$	$4.3^{+0.92}_{-0.75}$	$14.71^{+1.86}_{-1.65}$
LG	11	$4.15^{+0.5}_{-0.44}$	$5.62^{+2.2}_{-1.58}$	$12.33^{+4.12}_{-3.09}$
ALL/FOR	4	$3.07^{+1.22}_{-0.87}$	$2.6^{+0.37}_{-0.32}$	$12.63^{+7.65}_{-4.76}$

2.4. Geochronology

A representative sample of GD1 granodiorites (see below) was selected for in situ U-Pb zircon dating. Zircons were extracted from 3 to 4 kg of sample using conventional separation techniques. Hand-picked crystals were previously examined by Cathodoluminescence imaging using a Zeiss EVO50 SEM and subsequently analyzed for U and Pb isotopes by LA-SF ICP-MS techniques, using a Thermo-Scientific Element 2 XR sector field ICP-MS coupled to a New Wave UP-193 Excimer Laser System following the analytical protocol and data processing by Gerdes and Zeh (2006).

3. Anatomy of the Arbus Pluton

3.1. Petrography

The Arbus Pluton consists of a felsic core composed of cordierite-bearing leucogranites (LG units), rimmed by three pyroxene and hornblende-pyroxene-bearing granodioritic shells (GD1, GD2 and GD3). A small monzo-gabbroic intrusion (MG) recognized in the northern border zone predates the granodioritic shell (Figure 2). Field relationships and petrologic analyses indicate a general mafic to felsic evolution by crystal fractionation, with the leucocratic terms post-dating the granodiorites (Secchi et al., 1991). Geochronological data, obtained with different methods, indicate consistent ages. New U-Pb zircon dating of the chilled margin of GD1 granodiorites yield an age of 303.7 ± 1.1 Ma, which represents the emplacement age of the pluton (Figure 3). The previous Rb/Sr isochrones (309 ± 19 Ma) (Secchi et al., 1991) and Ar/Ar dating on late-stage muscovite (308 ± 1 Ma) (Boni, Stein, Zimmerman, & Villa, 2003) are in good agreement with the new LA-ICP-MS results.

The contact between Arbus Pluton and the basement is flat or gently dipping. In the northern part of the pluton, internal flat or gently dipping overall geometry is defined by the distribution of concordant sheets of different facies in GD3 (i.e. tourmaline microgranular granites and pegmatites: (GD3b) and porphyritic border facies: (GD3a)). Cognate dark enclaves of gabbroic and dioritic composition are common only in GD granodiorites; rare monzonitic enclaves are observed in the LG leucogranites. The size and abundance of enclaves in the granodiorites tends to increase southward being maximum in the GD2 granodiorites. Metamorphic xenoliths are particularly frequent in the GD1 granodiorites exposed along the northern sector of the pluton and, in general, are localized within a few meters of the contact with the basement. Both the xenoliths and enclaves show no evidence for plastic deformation of the primary mineral assemblage. Dyke swarms of acidic composition (Dmg), such as cordierite-bearing aplites and microgranites, are observed in the western part of Arbus Pluton; mafic dikes (Dlp), mainly spessartites, are rare.

3.2. Structural setting

The pluton emplaced at very shallow crustal levels within an E–W vertical shear zone that reactivated a segment of the frontal Variscan thrust. This structure is the foremost W-directed thrust which separates an allochthonous pile of lower greenschist units from a para-authoctonous foreland affected by very low-grade metamorphism (Funedda, 2009). Shallow crustal emplacement levels (2–4 km) are constrained by: (i) the occurrence of andalusite–cordierite–biotite contact aureole, the Al-in hornblende barometer in granodiorites (Anderson & Smith, 1995), which yield values close to about 1 Kb (Secchi et al., 1991). The hornfels zone reach a maximum thickness of about 1000 m along the southern border of the pluton, while it does not exceeds an apparent thickness of about 20–70 m northward. This difference depends on the geometry of the pluton, which is flat along the northern side and steep southward. Orientation data collected in about 100 different localities (see figure in the Main Map) indicate that the magmatic foliation defined by metamorphic xenoliths and mafic enclaves has a general E–W trend and is steeply dipping in the southern margin of the pluton. The fabric becomes almost flat in the central and northern part of the pluton, whereas close to the pluton border it tends to parallelize the contact with the country rocks, producing a locally steep and variably oriented pattern.

4. Faults and fractures

The Arbus Pluton has offset a network of late – to post-magmatic faults, probably reactivated several times from Early Permian to the Pliocene (Carmignani, Barca, et al., 1994). The main structures are N60°–80° dextral strike-slip faults injected by micro-granitic dykes and late-magmatic hydrothermal quartz veins. These structures are systematically displaced by NE–SW sinistral and NW–SE dextral conjugate faults with a clear down-dip component. However, these latter fault systems are associated with late-magmatic quartz veins and micro-granitic dykes, indicating that the different sets of faults must be substantially coeval.

5. Ore deposits

The study area hosts relevant examples of late-Variscan granite-related hydrothermal ore deposits. The most striking feature is represented by a narrow (0.5–3 km) hydrothermal vein system that can be traced for over 10 km around the Arbus Pluton. Veins fill steeply dipping (up to 70°–80°), peripheral, open fractures

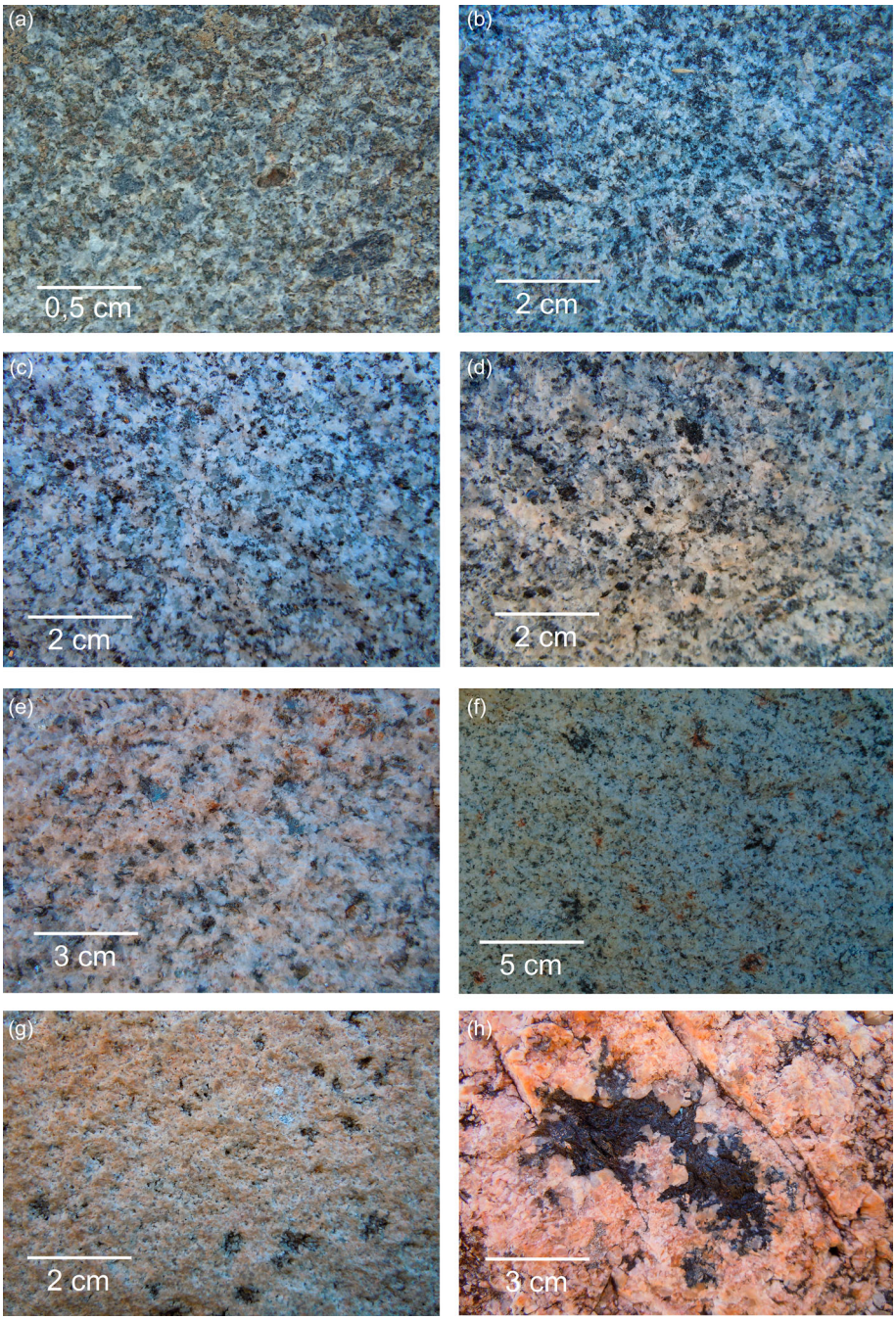

Figure 2. Macroscopic features of the main recognized intrusive facies: (a) leuco quartz – monzogabbronorites (MG); (b), (c) and (d) GD1, GD2 and GD3 granodiorites, respectively; (e), (f) and (g) LG1, LG2 and LG3 leucogranites, respectively with centimetric aggregates of cordierite and quartz; (h) tourmaline granites.

dipping sideways to the pluton margin. These structures represent dilatational jogs developed along late-Variscan normal faults during the cooling of the pluton. Close to the northern and western contacts of Arbus Pluton, a huge system of veins host one of the largest and richest Variscan Pb-Zn (Ag) ore deposits in Europe, having been mined for several centuries (Montevecchio–Ingurtosu–Gennamari district; (Cavinato & Zuffardi, 1948)). The veins are polymetallic associations of Pb-Zn (Cu, Ag) sulfides with accessory Ni-Co arsenides (Dessau, 1935), generally included in a quartz–siderite gangue. Complex ore/gangue relationships and minor changes in composition indicate a multi-stage hydrothermal process possibly linked to changes of source and physical parameter of the fluids. South from the contact with the Arbus Pluton, hydrothermal veins hosted in the foreland unit are smaller and more discontinuous. Ni-Co arsenides are dominant over Pb-Zn sulfides (Dessau, 1936). In this area, high-temperature (hypothermal) occurrences are documented as small swarms of Sn-As (W)-bearing quartz veins (Zuffardi, 1958). These NE–SW trending bodies are mostly sub-vertical. Moreover, a roughly E–W trending vein system cut across the Arbus Pluton and, locally, the acidic and mafic dikes. It consists of sub-vertical, N-dipping, quartz veins mineralized

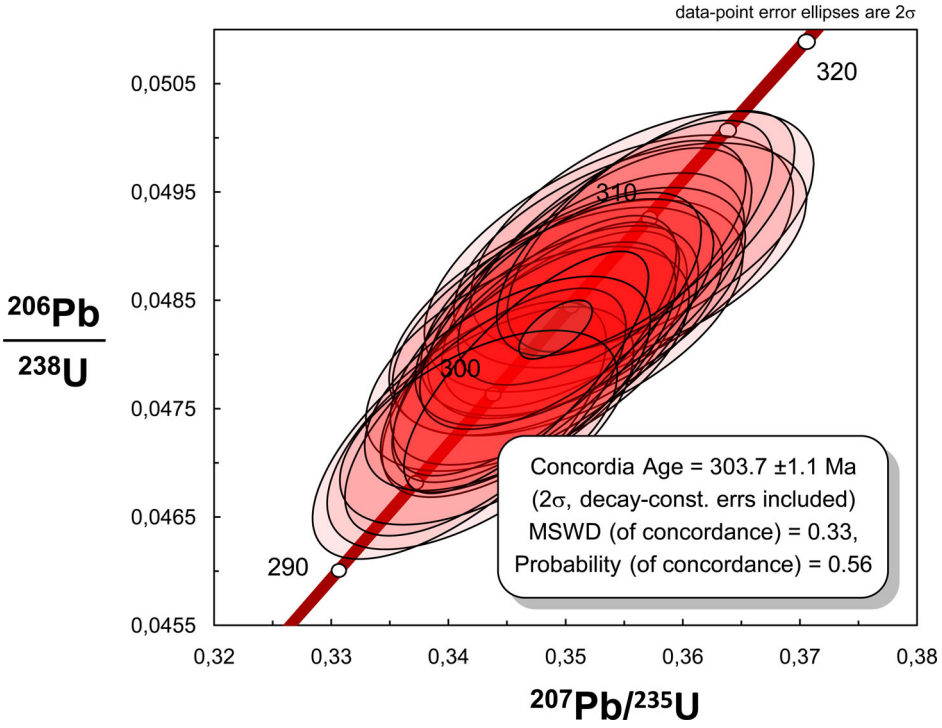

Figure 3. Wetherill concordia diagram of dated sample (GD1 facies).

with abundant Fe oxides (hematite, goethite) and minor Pb-Zn sulfides. Their wall rocks are frequently silicified and/or kaolinized. At Ingurtosu and Gennamari areas, this vein system offsets the peripheral veins. Finally, a very late system of NW-striking quartz veins, locally mineralized (Pb-F) occurs in the southern sector; it distinctly crosscuts all the previously described systems.

6. Conclusions

Structural constraints suggest that the Arbus Pluton was emplaced within a narrow E–W vertical shear zone that reactivated the frontal thrust as a strike-slip structure. The geometry of the pluton resembles an E–W trending elliptical body, as formerly argued by Cavinato (1930). The steep magmatic flow trajectories observed in the southern, relatively mafic, granodiorites can be interpreted as the feeder zone, possibly rooted in a crustal E–W shear zone. This interpretation is further supported by the occurrence of larger mafic enclaves as well as a lower U/Th ratio.

Relatively fast cooling processes in the uppermost crust in an active shear zone could explain the development of the peripheral system of fractures, while the structural framework and the geometry of the pluton favored the prevailing northward migration of hydrothermal fluids to repeatedly fill the fractures, producing the Montevecchio–Ingurtosu–Gennamari system. The metallogenic framework of the district may be explained in terms of polyphase evolution: an early high-temperature episode (Sn-As ores), followed by huge hydrothermal circulation in a mesothermal stage (Pb-Zn and Ni-Co ores (Honisch, 2008)), driven by tectonics along the intrusions/basement contact. A late, lower temperature stage is testified by the Fe oxides-bearing E–W system. Similar stable Pb isotope data in K-feldspars from the Arbus intrusives and in galenas from the Montevecchio mine area (Ludwig, Vollmer, Turi, Simmons, & Perna, 1989) may indicate that metals could have been mobilized by sub-solidus leaching of feldspars during the latest magmatic phases; at the same time, the presence of abundant Ni-Co ores close to the southern borders of the pluton may imply a possible source from mafic rocks at depth.

Disclosure statement

No potential conflict of interest was reported by the authors.

Software

The map was digitized using Esri ArcGIS 9.3. Matlab was used for the remote sensing analysis. The field spectrometric analysis was performed using jRadview (Caciolli et al., 2012). The isotopic composition of monazite grains was analyzed using the Glitter package (Van Achterberg, Ryan, Jackson, & Griffin, 2001). Concordia diagrams (2σ error ellipses) and concordia ages (95% confidence level) were produced using Isoplot/Ex 4 (Ludwig, 2012) 4 were used to elaborate U-Pb isotopic data on zircons.

References

Anderson, J. L., & Smith, D. R. (1995). The effects of temperature and fO2 on the Al-in-horneblende barometer. *American Mineralogist*, *80*, 549–559.

Boni, M., Stein, H. J., Zimmerman, A., & Villa, I. M. (2003). *Mineral exploration and sustainable development*.

Bralia, A., Ghezzo, C., Guasparri, G., & Sabatini, G. (1981). Aspetti genetici del batolite sardo-corso. *Rendiconti società italiana di mineralogia e petrografia*, *38*(2), 701–764.

Caciolli, A., Baldoncini, M., Bezzon, G. P., Broggini, C., Buso, G. P., Callegari, I., … Xhixha, G. (2012). A new FSA approach for in situ γ ray spectroscopy. *Science of the Total Environment*, *414*, 639–645. doi:10.1016/j.scitotenv.2011.10.071

Carmignani, L., Barca, S., Disperati, L., Fantozzi, P. L., Funedda, A., Oggiano, G., & Pasci, S. (1994). Tertiary compression and extension in the Sardinian basement. *Bollettino di Geofisica Teorica e Applicata*, *36*, 45–62.

Carmignani, L., Carosi, R., Di Pisa, A., Gattiglio, M., Musumeci, G., Oggiano, G., & Pertusati, P. C. (1994). The Hercynian chain in Sardinia (Italy). *Geodinamica Acta*, *7*(1), 31–47.

Casini, L., Cuccuru, S., Maino, M., Oggiano, G., Puccini, A., & Rossi, P. (2015). Structural map of Variscan northern Sardinia (Italy). *Journal of Maps*, *11*(1), 75–84. doi:10.1080/17445647.2014.936914

Casini, L., Cuccuru, S., Maino, M., Oggiano, G., & Tiepolo, M. (2012). Emplacement of the Arzachena Pluton (Corsica–Sardinia Batholith) and the geodynamics of incoming Pangaea. *Tectonophysics*, *544–545*, 31–49. doi:10.1016/j.tecto.2012.03.028

Casini, L., Cuccuru, S., Puccini, A., Oggiano, G., & Rossi, P. (2015). Evolution of the Corsica–Sardinia Batholith and late-orogenic shearing of the Variscides. *Tectonophysics*, *646*, 65–78. doi:10.1016/j.tecto.2015.01.017

Casini, L., Puccini, A., Cuccuru, S., Maino, M., & Oggiano, G. (2013). GEOTHERM: A finite difference code for testing metamorphic P–T–t paths and tectonic models. *Computers & Geosciences*, *59*, 171–180. doi:10.1016/j.cageo.2013.05.017

Cavinato, A. (1930). *Ricerche geologico-petrografiche sulla regione dell'Arburese-Sardegna*. Padova: Società Cooperativa Tipografica.

Cavinato, A., & Zuffardi, P. (1948). Geologia della miniera di Montevecchio. In Società Italiana Piombo Zinco (Ed.), *Notizie sull'industria del Piombo e dello Zinco* (pp. 431–464). Milano.

Cocherie, A., Rossi, P., Fanning, C. M., & Guerrot, C. (2005). Comparative use of TIMS and SHRIMP for U–Pb zircon dating of A-type granites and mafic tholeiitic layered complexes and dykes from the Corsican Batholith (France). *Lithos*, *82*(1–2), 185–219. doi:10.1016/j.lithos.2004.12.016

Dessau, G. (1935). Appunti sui giacimenti minerari di Gennamari-Ingurtosu. Bollettino della Societa Geologica Italiana, *54*, 229–240.

Dessau, G. (1936). I minerali dei filoni a nichelio e cobalto dell'Arburese (Sardegna). Periodico di Mineralogia, *7*, 21–39.

Ferré, E. C., & Leake, B. E. (2001). Geodynamic significance of early orogenic high-K crustal and mantle melts: Example of the Corsica Batholith. *Lithos*, *59*(1–2), 47–67. doi:10.1016/s0024-4937(01)00060-3

Friese, N., Vollbrecht, A., Tanner, D. C., Fahlbusch, W., & Weidemann, M. (2011). Multi-stage emplacement of the Götemar Pluton, SE Sweden: New evidence inferred from field observations and microfabric analysis, including cathodoluminescence microscopy. *International Journal of Earth Sciences*, *101*(5), 1149–1167. doi:10.1007/s00531-011-0739-y

Funedda, A. (2009). Foreland – And hinterland-verging structures in fold-and-thrust belt: An example from the Variscan foreland of Sardinia. *International Journal of Earth Sciences*, *98*(7), 1625–1642. doi:10.1007/s00531-008-0327-y

Gaggero, L., Oggiano, G., Buzzi, L., Slejko, F. F., & Cortesogno, L. (2007). Post-variscan mafic dikes from the late orogenic collapse to the Tethyan rift: Evidence from Sardinia. *Ofioliti*, *32*(1), 15–37.

Gerdes, A., & Zeh, A. (2006). Combined U–Pb and Hf isotope LA-(MC-)ICP-MS analyses of detrital zircons: Comparison with SHRIMP and new constraints for the provenance and age of an Armorican metasediment in Central Germany. *Earth and Planetary Science Letters*, *249*(1–2), 47–61. doi:10.1016/j.epsl.2006.06.039

Honisch, M. (2008). PbS-ZnS ore mineralization in SW Sardinia (Ingurtosu-Gennamari). Fluid inclusions invstigations. (Msthesis Lehrstuhl für Geologie und la gerstättenlehre), Montanistische universität Leoben (Austria).

Ludwig, K. R. (2012). *User's manual for Isoplot 3.75: A geochronological toolkit for Microsoft Excel*. Berkeley, CA: Berkeley Geochronological Center. Retrieved from http://www.bgc.org/isoplot_etc/isoplot/Isoplot3_75-4_15manual.pdf

Ludwig, K. R., Vollmer, R., Turi, B., Simmons, R. K., & Perna, G. (1989). Isotopic constraints on the genesis of base-metal ores in southern and central Sardinia. *European Journal of Mineralogy*, *1*(5), 657–666.

Maino, M., Casini, L., Ceriani, A., Decarlis, A., Di Giulio, A., Seno, S., … Stuart, F. M. (2015). Dating shallow thrusts with zircon (U-Th)/He thermochronometry – The shear heating connection. *Geology*, *43*(6), 495–498.

Paquette, J. L., Ménot, R.-P., Pin, C., & Orsini, J. B. (2003). Episodic and short-lived granitic pulses in a post-collisional setting: Evidence from precise U–Pb zircon dating through a crustal cross-section in Corsica. *Chemical Geology*, *198*(1–2), 1–20. doi:10.1016/s0009-2541(02)00401-1

Poli, G., Ghezzo, C., & Conticelli, S. (1989). Geochemistry of granitic rocks from the Hercynian Sardinia-Corsica batholith: Implication for magma genesis. *Lithos*, *23*(4), 247–266. doi:10.1016/0024-4937(89)90038-8

Puccini, A., Xhixha, G., Cuccuru, S., Oggiano, G., Xhixha, M. K., Mantovani, F., … Casini, L. (2014). Radiological characterization of granitoid outcrops and dimension stones of the Variscan Corsica-Sardinia Batholith. *Environmental Earth Sciences*, *71*(1), 393–405. doi:10.1007/s12665-013-2442-8

Rossi, P., & Cocherie, A. (1991). Genesis of a Variscan batholith: Field, petrological and mineralogical evidence from the Corsica-Sardinia batholith. *Tectonophysics*, *195*(2–4), 319–346.

Rossi, P., Oggiano, G., & Cocherie, A. (2009). A restored section of the 'southern Variscan realm' across the Corsica–Sardinia microcontinent. *Comptes Rendus Geoscience*, *341*(2–3), 224–238. doi:10.1016/j.crte.2008.12.005

Secchi, F. A., Brotzu, P., & Callegari, E. (1991). The Arburese igneous complex (SW Sardinia, Italy) – An example of dominant igneous fractionation leading to peraluminous cordierite-bearing leucogranites as residual melts. *Chemical Geology*, *92*(1–3), 213–249. doi:10.1016/0009-2541(91)90057-x

Van Achterberg, E., Ryan, C. G., Jackson, S. E., & Griffin, W. L. (2001). Data reduction software for LA-ICP-MS. In P. Sylvester (Ed.), *Laser ablation-ICPMS in the earth science* (pp. 239–243). Ottawa, Ontario, Canada: Mineralogical Association of Canada.

Zorpi, M. J., Coulon, C., & Orsini, J. B. (1991). Hybridization between felsic and mafic magmas in calc-alkaline granitoids; A case study in northern Sardinia, Italy. *Chemical Geology*, *92*, 45–86.

Zuffardi, P. (1958). Su nuova segnalazione di cassiterite in Sardegna e sulla presenza di tracce di stagno in alcuni adunamenti idrotermali sardi. *Rendiconti associazione mineralogica sarda*, *63*, 27–38.